

Self-force on extreme mass ratio inspirals via curved spacetime effective field theoryChad R. Galley^{1,*} and B. L. Hu^{1,2,†}¹*Maryland Center for Fundamental Physics, Department of Physics, University of Maryland, College Park, Maryland, 20742, USA*²*Perimeter Institute for Theoretical Physics, 31 Caroline Street North, Waterloo, Ontario, Canada N2L 2Y5*

(Received 5 June 2008; published 2 March 2009)

In this series we construct an effective field theory (EFT) in curved spacetime to study gravitational radiation and backreaction effects. We begin in this paper with a derivation of the self-force on a compact object moving in the background spacetime of a supermassive black hole. The EFT approach utilizes the disparity between two length scales, which in this problem are the size of the compact object r_m and the radius of curvature of the background spacetime \mathcal{R} such that $\varepsilon \equiv r_m/\mathcal{R} \ll 1$, to treat the orbital dynamics of the compact object, described as an effective point particle, separately from its tidal deformations. The equation of motion of an effective relativistic point particle coupled to the gravitational waves generated by its motion in a curved background spacetime can be derived without making a slow motion or weak field approximation, as was assumed in earlier EFT treatment of post-Newtonian binaries. Ultraviolet divergences are regularized using Hadamard's *partie finie* to isolate the nonlocal finite part from the quasilocal divergent part. The latter is constructed from a momentum space representation for the graviton retarded propagator and is evaluated using dimensional regularization in which only logarithmic divergences are relevant for renormalizing the parameters of the theory. As a first important application of this framework we explicitly derive the first-order self-force given by Mino, Sasaki, Tanaka, Quinn, and Wald. Going beyond the point particle approximation, to account for the finite size of the object, we demonstrate that for extreme mass ratio inspirals the motion of a compact object is affected by tidally induced moments at $O(\varepsilon^4)$, in the form of an effacement principle. The relatively large radius-to-mass ratio of a white dwarf star allows for these effects to be enhanced until the white dwarf becomes tidally disrupted, a potentially $O(\varepsilon^2)$ process, or plunges into the supermassive black hole. This work provides a new foundation for further exploration of higher order self-force corrections, gravitational radiation, and spinning compact objects.

DOI: [10.1103/PhysRevD.79.064002](https://doi.org/10.1103/PhysRevD.79.064002)

PACS numbers: 04.25.Nx, 04.30.Db, 04.62.+v

I. INTRODUCTION AND MAIN POINTS

In two previous papers [1,2] (see also [3]), using a stochastic field theory approach based on open system concepts, we derive the scalar, electromagnetic, and gravitational self-force to leading order on a particle moving in an arbitrary curved background spacetime. We begin with the particle following a quantum mechanical path while interacting with a linear quantum field [4–6]. The conditions on a stochastic field theory (for open systems) to emerge from a quantum field theory (of closed systems) are that the mass and size of the particle are large enough so the particle worldline is sufficiently decohered from its interactions with the quantum fluctuations of the field that it can be considered as quasiclassical, and yet sufficiently small that quantum fluctuations manifest as classical stochastic forces [7].

A. Quantum, stochastic, and effective field theories

When there is a significant discrepancy between the two mass (or energy or length) scales in a problem, as in the extreme mass ratio binary systems under consideration

here, one could use an open system stochastic description for their dynamics, such as developed in [1,2]. When this discrepancy is huge (such as between the QCD and GUT scales in particle physics), the stochastic component is strongly suppressed in the wide range between the two scales, away from the threshold region [8]. Then the stochastic field theory description will give rise to an effective field theory (EFT) description [9] for the motion of the small mass subsystem. Because of the large separation in the mass scales quantum loop corrections from the field and the intrinsic quantum mechanical worldline fluctuations are very strongly suppressed. These two factors render a quantum field theory (QFT) into a stochastic field theory (with sufficiently decohered histories) and in turn (with sufficiently small stochasticity) an effective field theory for the dynamics of the reduced systems. We shall explain the essence and demonstrate the advantages in taking a field theory approach to treat radiation-reaction of classical systems. The application of EFT to the treatment of gravitational radiation from post-Newtonian (PN) binary systems was first introduced by Goldberger and Rothstein [10]. Our formulation of a curved spacetime effective field theory (CS-EFT) goes beyond with two important features: it is for any curved spacetime background and there is no slow motion or weak field restrictions [11].

*crgalley@umd.edu

†blhu@umd.edu

In this and three subsequent papers [12–14] we construct a CS-EFT and apply it to derive the self-force on a compact object moving in an arbitrary curved background. For concreteness, the background spacetime is assumed to be that of a supermassive black hole (SMBH) with curvature scale \mathcal{R} much larger than the size of the compact object r_m . The smallness of the ratio $\varepsilon \equiv r_m/\mathcal{R}$ makes it a good expansion parameter for a perturbation theory treatment describing the extreme mass ratio inspiral (EMRI) of the compact object. These binary systems are expected to be good candidates for detecting gravitational wave signatures using the space-based gravitational wave interferometer LISA [15].

We emphasize that the formalism we construct here is of a sufficiently general nature that it can be applied to any compact object moving in an arbitrary curved background, including those spacetimes sourced by some form of stress energy and those possessing a cosmological constant.

B. Relevant scales in EMRIs

Consider the motion of a compact object (a black hole, neutron star, or white dwarf with a mass m ranging from about 1 to 100 solar masses) moving through the spacetime of a SMBH with a mass $M \sim 10^{5-7}M_\odot$. We have in mind that the compact object moves in a stationary background provided by the supermassive black hole, such as the Schwarzschild or Kerr spacetimes. Such spacetimes are appropriate for a description of the EMRI in which the compact object is bound by the gravitational pull of the SMBH. By emitting gravitational waves, the binary system loses energy until the compact object plunges into the SMBH. The emission of gravitational radiation from such a system is expected to be detected with the anticipated construction and launch of the LISA space-based interferometer [15].

It is believed that most SMBHs lurking in the middle of galaxies, which are thought to host the prime sources of gravitational wave emissions detectable by LISA, are spinning and clean in the sense that most, if not all, of the surrounding material has already fallen into the black hole. (Active galactic nuclei are a notable exception [16].) Because of this the Kerr background is perhaps the most astrophysically relevant spacetime for the extreme mass ratio inspiral. The Kerr solution is vacuum, stationary, and stable under small perturbations [17].

There are two relevant length scales in EMRIs. The smaller scale is set by the size of the compact object itself, denoted r_m . For an astrophysical black hole its radius is $r_{\text{bh}} = 2G_N m \sim m/m_{\text{pl}}^2$, where $m_{\text{pl}}^{-2} = 32\pi G_N$ in units where $\hbar = c = 1$ [18]. For a neutron star with a mass $\approx 1.4M_\odot$ and a radius of 10–16 km, it follows that $r_{\text{ns}} \approx 4.8\text{--}7.7G_N m \sim m/m_{\text{pl}}^2$. Therefore, it is to be expected that the size of the compact object, be it a black hole or a neutron star, is of the order of its mass [19].

The second relevant scale is the radius of curvature of the background spacetime, \mathcal{R} . We take \mathcal{R} to be the following curvature invariant:

$$\mathcal{R} = (R_{\mu\alpha\nu\beta}R^{\mu\alpha\nu\beta})^{-1/4}. \quad (1.1)$$

For a (possibly rotating) stationary SMBH the radius of curvature is $\mathcal{R} \sim (m_{\text{pl}}^2 r^3/M)^{1/2}$, where r is the typical orbital distance for the compact object away from the central black hole. For example, r is the geometric mean of the semimajor and semiminor axes of a compact object in an inclined elliptical orbit. In an approximately circular orbit r is the orbital radius, and for a particle moving faster than the escape velocity r is the impact parameter.

In the strong-field regime where $r \sim M/m_{\text{pl}}^2$, the curvature scale is also $\sim M/m_{\text{pl}}^2$ implying that $r/\mathcal{R} \sim m/M$ when a perturbative expansion in ε is equivalent to one in m/M .

The typical variation in time and space of the background is $\gtrsim \mathcal{R}$. The wavelength λ of radiated metric perturbations from the compact object in a bound orbit is $\lambda \sim \mathcal{R}$, which shows that the wavelength of the gravitational waves does not provide a separate scale independently from \mathcal{R} .

C. The CS-EFT approach: Issues and main features

The effective field theory approach was first introduced for the consideration of gravitational radiation from post-Newtonian binary systems in [10], spinning compact objects in [20–23], and dissipative effects due to the absorption of gravitational waves in [24,25]. See [26–28] for introductory reviews. Let us call these theories PN-EFT: they are constructed to describe the motion of two slowly moving compact objects in a *flat background*. In particular, the compact objects are treated as effective *point particles*, the worldlines of which carry nonminimal operators describing the multipole moments from companion-induced tidal deformations as well as possible spin degrees of freedom and other intrinsic moments. Below we describe briefly some general features of EFT and the specific differences between our new CS-EFT approach and the existing PN-EFT.

The use of point particles to source the metric perturbations about the flat background spacetime (note that the high frequency waves in a quantum description corresponds to massless spin-two particles, the gravitons, in flat space quantum field theory) prompts the appearance of divergences. Fortunately there exists a well-established bank of tools and techniques in quantum field theory for regularizing these divergences and renormalizing the parameters and coupling constants of the theory. A theory is renormalizable in the effective field theory sense if observables are calculated in the low energy limit: the divergences can always be absorbed into a renormalization of the coupling constants of the infinite number of nonminimal worldline operators. The use of dimensional regularization

is particularly useful in effective field theories because the renormalization group equations are mass independent for this scheme indicating that only logarithmic divergences contribute to the renormalization procedure [29].

Our CS-EFT approach differs from this group of work in two ways. First, we work with an arbitrary *curved spacetime*. Second, we allow for the compact object to move with *relativistic speeds* in *strong-field* regions of the background spacetime. The post-Newtonian effective field theory of [10] treats bodies moving slowly through a weak gravitational field.

1. In-in formulation for real and causal equations of motion

Technically there are also fundamental differences. In the in-out formalism (see, e.g., in the present context, [10]) the generating functional Z , given by

$$Z[j^\mu, J^{\mu\nu}] = \langle 0, \text{out} | 0, \text{in} \rangle_{j,J}, \quad (1.2)$$

yields the transition amplitude of the system from the vacuum state in the asymptotic past $|0, \text{in}\rangle$ to the vacuum state in the asymptotic future $|0, \text{out}\rangle$. The current densities j^μ and $J^{\mu\nu}$ couple linearly to the particle's worldline coordinate and the metric perturbation, respectively. In a curved or time-dependent spacetime or background field, $|0, \text{out}\rangle$ is in general different from $|0, \text{in}\rangle$ as a result of particle production and other quantum field processes owing to the changing background. The in-out generating functional Z yields matrix elements but not expectation values and the in-out effective action (obtained as the Legendre transform of Z) generates equations of motion for $\hat{z}^\mu(\tau)$ that are neither real nor causal in general [30].

In flat or stationary spacetimes where the in and out vacua are equal, one may think that such problems are moot. Even in these special geometries the in-out formalism fails to give real and causal equations of motion for the expectation value of the particle worldline coordinates. The reason for this is as follows. To compute the effective action the field is integrated out from the transition amplitude Z . In the process, certain boundary conditions are imposed on the structure of the field modes in the asymptotic past and future. In the in-out formulation, which is useful for the calculation of scattering amplitudes, one often chooses the Feynman propagator as the appropriate Green's function thereby giving the radiation and particle dynamics a nonretarded structure. For the EMRI case under study, using the in-out formalism, the leading order gravitational perturbation from (A18) is given by

$$\begin{aligned} & \text{Re} \left[\frac{im}{2m_{\text{pl}}} \int d\tau D_{\mu\nu\alpha\beta}^F(x, z^\mu) u^\alpha u^\beta \right] \\ &= \frac{m}{4m_{\text{pl}}} \int d\tau [D_{\mu\nu\alpha\beta}^{\text{ret}}(x, z^\mu) + D_{\mu\nu\alpha\beta}^{\text{adv}}(x, z^\mu)] u^\alpha u^\beta, \end{aligned} \quad (1.3)$$

which includes radiation from the source in the future. At higher orders in perturbation theory the problems become worse due to the appearance of nonlocal integrations that manifest even in flat spacetime.

It is possible to construct true expectation values within the in-out formalism by summing over a set of complete states in the asymptotic future so that, for example, the graviton one-point function is

$$\langle 0, \text{in} | \hat{h}_{\mu\nu} | 0, \text{in} \rangle = \sum_{\alpha} \langle 0, \text{in} | \alpha, \text{out} \rangle \langle \alpha, \text{out} | \hat{h}_{\mu\nu} | 0, \text{in} \rangle.$$

This construction requires knowing the Bogoliubov coefficients $\langle 0, \text{in} | \alpha, \text{out} \rangle$, which relate the in vacuum to the out states. Even in spacetimes with isometries these can be quite difficult to compute and do not necessarily have simple functional forms. Having computed these coefficients, one still needs to perform the sum over intermediate final states making this a demanding calculation all around.

The proper procedures described above are systematically accounted for in the in-in [or closed-time-path (CTP) or Schwinger-Keldysh] formalism [31–36]. The in-in or CTP generating functional is defined as

$$Z[j_1^\mu, j_2^\mu, J_1^{\mu\nu}, J_2^{\mu\nu}] = \sum_{\alpha} \langle 0, \text{in} | \alpha \rangle_{j_2, J_2} \langle \alpha | 0, \text{in} \rangle_{j_1, J_1}, \quad (1.4)$$

where $\{\alpha\}$ forms any complete set of states on a constant-time hypersurface $\Sigma(T)$ at some possibly finite time T . See Fig. 1. Within this framework we do not need to know the states at the asymptotic future since only the initial states on a constant-time hypersurface in the asymptotic past need to be specified. As such, the in-in formalism is an initial value formulation (rather than a boundary value formulation, as contained in the in-out formalism) of quan-

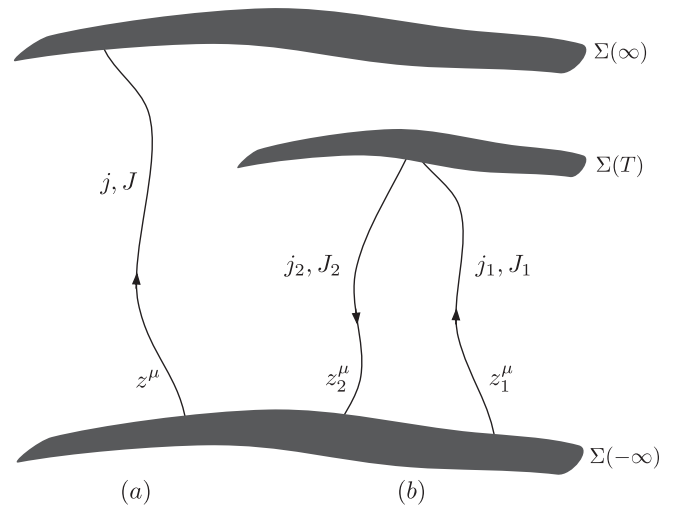


FIG. 1. A cartoon representation of (a) the in-out vacuum transition amplitude and (b) the in-in (or CTP) generating functional. In the in-in formalism the currents and trajectories are set equal to each other at the end of a calculation to obtain equations of motion, physical observables, etc.

tum field theory. The CTP effective action produces real and causal equations of motion and true expectation values of correlations [34,36]. For example, using the in-in formalism the leading order gravitational perturbation is causally propagated from the source to the field point

$$\frac{m}{2m_{\text{pl}}} \int d\tau D_{\mu\nu\alpha\beta}^{\text{ret}}(x, z^\mu) u^\alpha u^\beta, \quad (1.5)$$

in contrast to (1.3).

The in-in functional (or CTP integral) formalism (1.4) is therefore the correct framework for describing the causal dynamics of the relativistic particle and the gravitational radiation, and it is what we shall use in this series of papers.

2. Effective point particle description

Another important ingredient in our construction is an effective point particle description for the motion of the compact object. Going beyond the point particle approximation is necessary to include the effects of tidal deformations induced by the background curvature as well as the effects from spin and other intrinsic moments. Following [10], we introduce all possible terms into the point particle action that are consistent with general coordinate invariance and reparametrization invariance [and invariance under $SO(3)$ rotations for a nonspinning spherically symmetric compact object].

By implementing a matching procedure using coordinate invariant observables we can match the observables of the effective point particle theory with the long-wavelength limit of observables in the full “microscopic” theory to determine the values of the coupling constants of the non-minimal terms. As we will show in Sec. IV, this allows us to deduce the order at which finite size effects affect the motion of the compact object through the statement of an *effacement principle*. To our knowledge this has not been explicitly given in the literature before for the EMRI scenario.

3. The power counting rules

Power counting is a generalization of dimensional analysis. In our perturbative treatment it is crucial for determining how the Feynman rules scale with the parameter ε . Once the scaling of the Feynman rules are known we determine all of the tree-level Feynman diagrams that appear at a particular order. Those diagrams containing graviton loops are safely ignored. We also assemble the diagrams that include the nonminimal worldline operators describing the finite size of the compact object. Significantly, this allows us to determine the order in ε at which finite size effects enter the particle equations of motion.

With the power counting rules, the EFT approach becomes an efficient and systematic framework for calculating the self-force to any order in perturbation theory.

Furthermore, by knowing how each Feynman diagram scales with ε , we can study a particular physical interaction that is of interest by focusing our attention on a single diagram or on a few diagrams without having to calculate every contribution that appears at that order and at lower orders. For example, the leading order spin-spin interaction (spin here refers to that of the compact object, not of the SMBH) contributes to the self-force at third order in ε for a maximally rotating compact object and can be calculated from the appropriate Feynman diagram [3,14]. The power counting rules, the Feynman rules, and their scaling with ε are derived in Secs. III B and III C.

4. Divergences and regularization

In Sec. III D we propose a method for regularizing the divergences in the effective action that is applicable at higher orders in perturbation theory. Our approach utilizes a mixture of distributional and momentum space techniques within the context of dimensional regularization. We know from previous work that the finite part of the self-force is generally nonlocal and history dependent. However, the ultraviolet divergences are quasilocal and independent of the history of the effective point particle’s motion. To isolate the quasilocal divergence from the non-local finite part, we use the method of Hadamard’s *partie finie*, or finite part, from distribution theory. (See Appendix B for a brief review of the definitions and concepts of distribution theory relevant in this work.)

After isolating the divergence from the nonlocal, finite remainder we then use a momentum space representation for the propagator in a curved background, first derived for a scalar field by Bunch and Parker [37], to calculate the divergent contributions. Their method is straightforward but not efficient for higher spin fields, including gravitons in a curved space. (See also the related work of [38].)

A novel method applicable for any tensor field is developed in [39] for computing the momentum space representation of the Feynman propagator. The method is sufficiently general to do the same for any quantum two-point function, including the retarded propagator $D_{\alpha\beta\gamma\delta}^{\text{ret}}(x, x')$. This approach makes use of diagrammatic techniques borrowed from perturbative quantum field theory. In Riemann normal coordinates, we expand the field action in terms of the displacement from the point x . The series can be represented in terms of Feynman diagrams, which allows for an efficient evaluation of each term in the expansion. Furthermore, we prove that some of the diagrams are zero to all orders. This identity is not recognized in [37] even though its relation to certain steps made in their calculations is evident.

D. MST-QW equation

Assembling all these essential ingredients, in Sec. III we give a demonstration of how the curved spacetime effective field theory construction is implemented, outline the steps

in the regularization of divergences, perform an actual calculation of the effective action, and from it derive the equation of motion for the compact object including the effect of gravitational self-force. As an application we work to first order in the mass ratio (i.e., ϵ) and obtain the well-known Mino-Sasaki-Tanaka-Quinn-Wald (MST-QW) equation [40,41]. This also sets the stage for calculating the second order self-force, the emitted gravitational waves, and the motion of compact objects with spin [12–14].

II. EFFECTIVE FIELD THEORY FOR POST-NEWTONIAN BINARIES AND EMRIS

Before proceeding to construct a curved spacetime effective field theory for extreme mass ratio inspirals, we briefly summarize the original work of [10], which introduces effective field theory techniques for describing post-Newtonian binary sources of gravitational radiation.

A. EFT in flat space for post-Newtonian binaries

The aim of [10] is to describe the motion of two slowly moving bodies through a weak gravitational field using effective field theory techniques in order to generate a perturbative expansion in powers of the relative velocity. One of the many benefits of using an effective field theory approach is that the method is systematic and efficient so that there is in principle no obstacle calculating to any order in the velocity.

The authors in [10] start by replacing the compact objects with effective point particles. These are described by an action consisting of the usual point particle action plus all possible self-interaction terms that are consistent with general coordinate invariance and reparametrization invariance of the worldline. Then, the in-out generating functional is introduced to derive an effective action,

$$\exp\{iS_{\text{eff}}[z]\} \equiv \int \mathcal{D}h_{\mu\nu} \exp\{iS_{pp}[z, \eta + h] + iS[\eta + h]\}, \quad (2.1)$$

where S_{pp} is the effective point particle action, $S[\eta + h]$ is the Einstein-Hilbert action for the full spacetime metric, and z^α are the coordinates of the particle worldline.

Before integrating out the metric perturbations, the authors observe that it is useful to separate $h_{\mu\nu}$ into potential $H_{\mu\nu}$ and radiation $\bar{h}_{\mu\nu}$ contributions:

$$h_{\mu\nu} = H_{\mu\nu} + \bar{h}_{\mu\nu}. \quad (2.2)$$

This is suggested by the fact that the slowly moving bodies see a nearly instantaneous gravitational potential and yet radiate gravitational waves due to their relative accelerations. This decomposition is also required to make the Feynman diagrams all scale homogeneously with the rela-

tive velocity, v . In this way, the perturbative expansion in v is consistent and can be constructed to any order.

Integrating out the potential gravitons using perturbation theory yields a theory of point particles moving in potentials. The radiation gravitons and the particle worldlines are nondynamical at this stage and can be treated as external sources. In this effective theory, valid at the orbital scale of the binary, the authors derive the Einstein-Infeld-Hoffman potential [42] as a check of their method.

The last effective theory the authors have constructed involves integrating out the radiation gravitons. They then derive the famous power spectrum for quadrupolar gravitational radiation by calculating the first nonvanishing contribution to the imaginary part of the effective action; the real part of the effective action generates equations of motion while the imaginary part is related to the power of the emitted gravitational radiation.

Using an effective field theory approach, it is not too surprising that some of the parameters of the theory undergo classical renormalization group (RG) scaling. In fact, the appearance of such RG scaling is used by the authors to show that there are no finite size effects up to v^6 order. In their words, “whenever one encounters a log divergent integral at order v^6 in the potential, one may simply set it to zero. Its value cannot affect physical predictions.” [10]. This is how they resolve the problem of the undetermined regularization parameters that appear, at third post-Newtonian order, from regularizing the singular integrals encountered with the traditional PN expansion techniques. See [43] and references therein for a complete discussion of the regularization ambiguity.

B. EFT in curved spacetime for EMRIs

Our construction of an EFT does not rely on the slow motion of the bodies nor on the assumption that they move through a weakly curved region of spacetime. Quite the contrary, we allow for the compact object to move relativistically through the strong-field region of the SMBH background spacetime. As a result, the metric perturbations generated by the motion of the compact object cannot be partitioned simply into an instantaneous potential and radiation contributions.

Utilizing the dissimilar magnitudes of the compact object’s size and the background curvature scale, we can construct two kinds of effective field theories. The first describes the compact object, in isolation from other external sources, as an effective point particle, and the second comes from integrating out the long-wavelength gravitational perturbations. The resulting theory is that of an effective point particle subjected to a self-force from the gravitational radiation reaction as a result of its motion in the background spacetime, with the force and the radiation evolving self-consistently. Using a matching procedure we can establish the values of the coupling constants appearing in the effective point particle action.

C. EFT of a compact object

In applying the EFT formalism we first construct an effective point particle theory for the compact object with mass m . This allows for a point particle description of the compact object's motion through the background spacetime while taking into account any tidally induced moments, or finite size effects, that might affect its motion. An example is provided in classical electromagnetism wherein long-wavelength radiation scatters off a small, metallic sphere possessing no residual charge. The interaction of the field induces a time-varying dipole moment on the surface of the sphere. Since the wavelength is much larger than the sphere, this system can effectively be described by radiation interacting with a point particle carrying an induced dipole moment on its worldline.

The effective point particle description of the compact object is constructed by “integrating out” the short wavelength gravitational perturbations up to the scale $r_m \sim m/m_{\text{pl}}^2$. In doing so, we describe the motion of the compact object moving in the combined geometry (with metric $\bar{g}_{\mu\nu}$) of the background SMBH plus long-wavelength gravitational perturbations by the action

$$S_{\text{tot}} = S[\bar{g}] + S_{pp}[z, \bar{g}]. \quad (2.3)$$

Here $z^\alpha(\lambda)$ are the coordinates of the particle worldline and λ is its affine parametrization.

Being a description of the extended compact object, the effective point particle action should include all possible self-interaction terms that are consistent with the symmetries of the theory [9], which are general coordinate invariance and worldline reparametrization invariance. For the discussion here, we will assume that the compact object is perfectly spherical when removed from external influences (e.g. background curvature) so that it carries no permanent moments. This implies, for example, excluding spinning compact objects in our construction, at least for now [44]. Hence, S_{pp} should also be invariant under $SO(3)$ rotations.

Such a general action contains many terms that are redundant and can therefore be eliminated from the effective point particle action [45,46]. In this theory, the terms involving the Ricci curvature tensor and scalar can be removed from S_{pp} leaving

$$S_{pp}[z, \bar{g}] = -m \int d\tau + c_E \int d\tau \mathcal{E}_{\mu\nu} \mathcal{E}^{\mu\nu} + c_B \int d\tau \mathcal{B}_{\mu\nu} \mathcal{B}^{\mu\nu} + \dots, \quad (2.4)$$

which was first shown in [10]. The symmetric and traceless tensors $\mathcal{E}_{\mu\nu}$ and $\mathcal{B}_{\mu\nu}$ are the electric and magnetic parts of the Weyl curvature, defined as

$$\mathcal{E}_{\mu\nu} = C_{\mu\alpha\nu\beta} \dot{z}^\alpha \dot{z}^\beta \quad (2.5)$$

$$\mathcal{B}_{\mu\nu} = \epsilon_{\mu\alpha\beta\lambda} C^{\alpha\beta}{}_{\nu\rho} \dot{z}^\lambda \dot{z}^\rho, \quad (2.6)$$

where \dot{z}^α is the particle's 4-velocity.

The terms containing the square of the Riemann curvature (and higher powers) represent tidal effects on the compact object that are induced by the spacetime curvature. This is seen by noting that the equations of motion no longer have vanishing acceleration so that the effective point particle does not move along a geodesic of the spacetime,

$$ma^\mu(\tau) = 2c_E \mathcal{E}_{\alpha\beta} \mathcal{E}^{\alpha\beta;\mu} + \dots \quad (2.7)$$

Such deviation from geodesic motion is typical of tidally distorted bodies. We will show in a later section that these tidal effects will affect the motion of a black hole or neutron star at $O(\epsilon^4)$ in perturbation theory.

In the next section we derive the first-order equations of motion for the compact object using the CS-EFT approach. These equations, which describe the self-force on the mass m , were previously found by Mino, Sasaki, and Tanaka [40] using matched asymptotic expansions and independently by Quinn and Wald [41] using axiomatic methods. In principle, we can compute the formal equations of motion to higher orders in ϵ thereby extending the work of [40,41]. The second paper in this series [12] will give results through the second order in ϵ .

III. CS-EFT DERIVATION OF MST-QW EQUATION FOR FIRST-ORDER SELF-FORCE

In the previous section, we outlined the construction of an effective field theory that replaces the extended compact object by an effective point particle. In this section we construct an EFT for the motion of the effective particle by integrating out the metric perturbations at the scale of the radius of curvature \mathcal{R} . In doing so, we derive the MST-QW self-force on the compact object.

Denote the background (unperturbed) metric by $g_{\mu\nu}$ so that $\bar{g}_{\mu\nu}$ is given by the background geometry plus the perturbations generated by the presence of the moving compact object:

$$\bar{g}_{\mu\nu} = g_{\mu\nu} + \frac{h_{\mu\nu}}{m_{\text{pl}}}. \quad (3.1)$$

The metric perturbations $h_{\mu\nu}$ are presumed to be small so that $|h_{\mu\nu}| \ll m_{\text{pl}}$. We will occasionally make use of the shorthand notation $\bar{h}_{\mu\nu} = h_{\mu\nu}/m_{\text{pl}}$ for the (dimensionless) ratio of the metric perturbation to the Planck mass. From (2.3) the total action describing the interactions between the metric perturbations and the particle is given by the sum of the Einstein-Hilbert and effective point particle actions,

$$S_{\text{tot}}[g + \bar{h}, z] = S[g + \bar{h}] + S_{pp}[g + \bar{h}, z]. \quad (3.2)$$

We expand the Einstein-Hilbert action in orders of $h_{\mu\nu}$:

$$\begin{aligned}
 S[g + \bar{h}] &= \sum_{n=2}^{\infty} \frac{1}{n!} \int d^4x_1 \cdots d^4x_n h_{\alpha_1\beta_1} \cdots h_{\alpha_n\beta_n} \\
 &\quad \times V^{(n)\alpha_1\cdots\beta_n}(x_1, \dots, x_n) \\
 &\equiv S^{(2)} + S^{(3)} + \dots,
 \end{aligned} \tag{3.3}$$

where $S^{(n)}$ denotes the part of the action containing terms proportional to n factors of $h_{\mu\nu}$. The quadratic contribution is the kinetic term for $h_{\mu\nu}$ and provides the propagator corresponding to some appropriate boundary conditions (e.g., retarded, Feynman). The action is invariant under infinitesimal coordinate transformations on the background spacetime.

We also need to expand the point particle action in powers of $h_{\mu\nu}$. Using (2.4) we find

$$\begin{aligned}
 S_{pp}[z, g + \bar{h}] &= \sum_{n=0}^{\infty} \frac{1}{n!} \int d^4x_1 \cdots d^4x_n h_{\alpha_1\beta_1} \cdots h_{\alpha_n\beta_n} \\
 &\quad \times V_{pp}^{(n)\alpha_1\cdots\beta_n}(x_1, \dots, x_n) \\
 &\equiv S_{pp}^{(0)} + S_{pp}^{(1)} + S_{pp}^{(2)} + \dots,
 \end{aligned} \tag{3.4}$$

$$\begin{aligned}
 Z[j_1^\mu, j_2^\mu, J_1^{\mu\nu}, J_2^{\mu\nu}] &= \int \mathcal{D}z_1^\mu \mathcal{D}z_2^\mu \mathcal{D}h_1^{\mu\nu} \mathcal{D}h_2^{\mu\nu} \exp\left\{iS[g + \bar{h}_1] - iS[g + \bar{h}_2] + iS_{pp}[z_1, g + \bar{h}_1] - iS_{pp}[z_2, g + \bar{h}_2]\right. \\
 &\quad \left. + i \int d\lambda (j_{1\mu} z_1^\mu - j_{2\mu} z_2^\mu) + i \int d^4x g^{1/2} (J_{1\mu\nu} h_1^{\mu\nu} - J_{2\mu\nu} h_2^{\mu\nu})\right\},
 \end{aligned} \tag{3.6}$$

where the conditions $z_1^\mu = z_2^\mu$ and $h_1^{\mu\nu} = h_2^{\mu\nu}$ are met on the constant-time hypersurface where the complete set of intermediate states $\{|\alpha\rangle\}$ are summed over as in (1.4).

To guarantee a well-defined graviton propagator on the background spacetime, we adopt the Faddeev-Popov [47] gauge-fixing procedure by introducing the action

$$S_{\text{gf}} = -m_{\text{pl}}^2 \int d^4x g^{1/2} G_\alpha G^\alpha, \tag{3.7}$$

which is equivalent to picking the gauge $G_\alpha[h_{\mu\nu}] \approx 0$ for the metric perturbations. (The \approx denotes weak equality in the sense of Dirac [48].) Since we will be dealing with tree-level interactions only, there is no need to introduce ghost fields into the gravitational action.

We choose the Lorenz gauge for the trace-reversed metric perturbations, defined as

$$\psi_{\alpha\beta} \equiv h_{\alpha\beta} - \frac{1}{2} g_{\alpha\beta} h, \tag{3.8}$$

so that the gauge-fixing function is $G_\alpha[h_{\mu\nu}] = \psi_{\alpha\beta}{}^{;\beta}$. In this gauge, the leading order (kinetic) term in (3.3) is

$$\begin{aligned}
 S^{(2)} &= -\frac{1}{2} \int d^4x g^{1/2} \left(h_{\alpha\beta;\gamma} h^{\alpha\beta;\gamma} - \frac{1}{2} h_{;\alpha} h^{;\alpha} \right. \\
 &\quad \left. - 2h^{\alpha\beta} R_{\alpha\gamma\beta\delta} h^{\gamma\delta} \right).
 \end{aligned} \tag{3.9}$$

where $S_{pp}^{(n)}$ denotes the part of the action for the point particle containing terms proportional to n factors of $h_{\mu\nu}$. The leading order term is the usual point particle action $S_{pp}^{(0)} = -m \int d\tau$ and the first vertex operator is

$$V_{pp}^{(1)\alpha\beta}(x) = \frac{m}{2m_{\text{pl}}} \int d\lambda \frac{\delta^4(x-z)}{g^{1/2}} \frac{\dot{z}^\alpha \dot{z}^\beta}{(-g_{\mu\nu} \dot{z}^\mu \dot{z}^\nu)^{1/2}}, \tag{3.5}$$

which is the point particle stress tensor.

A. The closed-time-path effective action

The construction of an effective field theory for the point particle motion in a curved spacetime begins from (1.4) with a path integral representation for the CTP, or in-in, generating functional

Perturbation theory in the in-in formalism is formulated similar to that in the in-out formalism. In particular, the generating functional can be written as

$$\begin{aligned}
 Z[j_{1,2}^\mu, J_{1,2}^{\mu\nu}] &= \int \mathcal{D}z_1^\mu \mathcal{D}z_2^\mu \exp\left\{iS_{pp}^{(0)}[z_1] - iS_{pp}^{(0)}[z_2]\right. \\
 &\quad \left. + i \int d\lambda (j_{1\mu} z_1^\mu - j_{2\mu} z_2^\mu) \right. \\
 &\quad \left. + i \int d^4x \mathcal{L}_{\text{int}} \left[z_1^\mu, z_2^\mu, -i \frac{\delta}{\delta J_1^{\alpha\beta}}, -i \frac{\delta}{\delta J_2^{\alpha\beta}} \right] \right\} \\
 &\quad \times Z_0[J_{1,2}^{\mu\nu}],
 \end{aligned} \tag{3.10}$$

which is expressed as a certain functional derivative operator acting on a Gaussian functional of the external currents $J_{1,2}^{\mu\nu}$ and where the interaction Lagrangian is

$$\begin{aligned}
 \int d^4x \mathcal{L}_{\text{int}} &= \sum_{n=1}^{\infty} (S_{pp}^{(n)}[z_1, \bar{h}_1] - S_{pp}^{(n)}[z_2, \bar{h}_2]) \\
 &\quad + \sum_{n=3}^{\infty} (S^{(n)}[\bar{h}_1] - S^{(n)}[\bar{h}_2]).
 \end{aligned} \tag{3.11}$$

The quantity Z_0 is the free field generating functional for the metric perturbations

$$Z_0[J_{1,2}^{\mu\nu}] = \int \mathcal{D}h_1^{\mu\nu} \mathcal{D}h_2^{\mu\nu} \exp\left\{iS^{(2)}[\bar{h}_1] - iS^{(2)}[\bar{h}_2] + i \int d^4x g^{1/2} (J_{1\mu\nu} h_1^{\mu\nu} - J_{2\mu\nu} h_2^{\mu\nu})\right\} \quad (3.12)$$

and is calculated by integrating the Gaussian along the CTP contour giving

$$Z_0[J_{\pm}^{\mu\nu}] = \exp\left\{-\frac{1}{2} J_a^{\alpha\beta} \cdot D_{\alpha\beta\gamma'\delta'}^{ab} \cdot J_b^{\gamma'\delta'}\right\}, \quad (3.13)$$

where a \cdot denotes spacetime integration, $\int d^4x g^{1/2}(x)$. In this expression we introduce the averaged and differenced variables

$$J_{\pm}^{\mu\nu} = J_1^{\mu\nu} - J_2^{\mu\nu} \quad (3.14)$$

$$J_+^{\mu\nu} = \frac{1}{2}(J_1^{\mu\nu} + J_2^{\mu\nu}) \quad (3.15)$$

so that the matrix of free graviton two-point functions (in the so-called Keldysh representation [32]) is

$$D_{\alpha\beta\gamma'\delta'}^{ab}(x, x') = \begin{pmatrix} 0 & -iD_{\alpha\beta\gamma'\delta'}^{\text{adv}} \\ -iD_{\alpha\beta\gamma'\delta'}^{\text{ret}} & \frac{1}{2}D_{\alpha\beta\gamma'\delta'}^H \end{pmatrix}, \quad (3.16)$$

where $a, b = \pm$ and $D_{\alpha\beta\gamma'\delta'}^{++} = 0$. Specifically, these are the retarded/advanced propagators and the Hadamard two-point function. See Appendix A for their definitions, identities, and useful relations. The indices a, b are raised and lowered by the ‘‘CTP metric’’

$$c_{ab} = c^{ab} = \begin{pmatrix} 0 & 1 \\ 1 & 0 \end{pmatrix}. \quad (3.17)$$

Momentarily leaving out the tensor indices, $D_{cd} = c_{ca}c_{db}D^{ab}$ and $J_{\pm} = J^{\mp}$, etc.

Computing the partial Legendre transform of the generating functional with respect to the particle current gives the effective action

$$\Gamma[\langle \hat{z}_{\pm}^{\mu} \rangle, J_{\pm}^{\mu\nu}] = W[j_{\pm}^{\mu}, J_{\pm}^{\mu\nu}] - \int d\lambda j_{\mu}^a \langle \hat{z}_{\pm}^{\mu} \rangle, \quad (3.18)$$

where $W = -i \ln Z$. The equations of motion for the expectation values of the worldline coordinates are then found by varying the effective action,

$$0 = \frac{\delta \Gamma}{\delta \langle \hat{z}_{\pm}^{\mu} \rangle} \Big|_{z_{-}=0, z_{+}=z, j_{\pm}=J_{\pm}=0}. \quad (3.19)$$

The gravitational waves radiated by the compact object can be computed from the graviton one-point function

$$\langle \hat{h}_{\mu\nu}(x^{\alpha}) \rangle = \langle \hat{h}_{+\mu\nu}(x^{\alpha}) \rangle|_{z_{-}=0, z_{+}=z, j_{\pm}=J_{\pm}=0} \quad (3.20)$$

$$= \frac{\delta W}{\delta J_{\pm}^{\mu\nu}(x^{\alpha})} \Big|_{z_{-}=0, z_{+}=z, j_{\pm}=J_{\pm}=0} \quad (3.21)$$

and will be discussed further in [13].

Before calculating the effective action we make a few remarks. A classical equation of motion does not adequately describe the particle’s motion when the quantum mechanical fluctuations of the worldline are not negligible. However, the particle’s quantum trajectories can be decohered by interactions with the quantum fluctuations of the metric perturbations, or other matter fields present, resulting in a classical worldline for the particle. We call this the semiclassical limit (classical particle in a quantum field). The condition for the existence of a semiclassical limit and the appearance of stochastic behavior are stated in the beginning of the Introduction. See [1,2] and references therein for more details of the issues pertaining to a particle moving in an arbitrary curved background.

B. Power counting rules

The interaction terms $S^{(n>2)}$ and $S_{pp}^{(n>0)}$ represent self-interactions of the field and various particle-field interactions, respectively. Each of these terms may be represented by a Feynman diagram. To write down all of the relevant diagrams that contribute to the effective action at a specific order in ε , we need to know how each of the interaction terms scale with ε and \mathcal{R} . The scaling behaviors that we develop here are called power counting rules and are essentially a generalization of dimensional analysis. We first develop the power counting rules for the parameters of the effective field theory; we ignore for now the nonminimal point particle couplings in S_{pp} (i.e., c_E, c_B, \dots).

As discussed previously, the curvature scale \mathcal{R} describes the length scale of temporal and spatial variations of the curvature in the background geometry. This implies that each of the spacetime coordinates scale according to

$$x^{\mu} \sim \mathcal{R}. \quad (3.22)$$

From the kinetic term for the metric perturbations we deduce that if $S^{(2)} \sim 1$ then

$$1 \sim \mathcal{R}^4 h^2 \left(\frac{1}{\mathcal{R}}\right)^2 \sim \mathcal{R}^2 h^2 \quad (3.23)$$

and the metric perturbation scales with \mathcal{R} as

$$h_{\mu\nu} \sim \frac{1}{\mathcal{R}}. \quad (3.24)$$

The particle-field interactions, indicated by the terms $S_{pp}^{(n)}$ for $n \geq 1$, contain inverse powers of the Planck mass, m_{pl} . To power count these terms we form the ratio

$$\frac{m}{m_{\text{pl}}} \sim \left(\frac{m}{m_{\text{pl}}^2 \mathcal{R}}\right) \left(\frac{m_{\text{pl}}}{m}\right) (m\mathcal{R}). \quad (3.25)$$

The factor $m\mathcal{R}$ is the scale of the (conserved) angular momentum for a test particle following a geodesic in the strong-field region of the background spacetime [49] since

$$L = m g_{\alpha\beta} \psi^{\alpha} \dot{x}^{\beta} \sim m\mathcal{R}, \quad (3.26)$$

TABLE I. Power counting rules.

x^μ	$h_{\mu\nu}$	L	$\frac{m}{m_{\text{pl}}}$	$S_{pp}^{(n)}$	$S^{(n)}$
\mathcal{R}	$\frac{1}{\mathcal{R}}$	$m\mathcal{R}$	$\sqrt{\varepsilon L}$	$\varepsilon\left(\frac{L}{\varepsilon}\right)^{1-n/2}$	$\left(\frac{L}{\varepsilon}\right)^{1-n/2}$

where \dot{x}^β is the 4-velocity of the geodesic. We therefore find that

$$\frac{m}{m_{\text{pl}}} \sim \sqrt{\varepsilon L}. \quad (3.27)$$

The four scaling laws in (3.22), (3.24), (3.26), and (3.27) determine the power counting rules for identifying the appropriate Feynman diagrams that enter into the evaluation of the effective action. See Table I.

We now turn our attention to power counting the interaction terms in (3.10). We consider first the diagram for the interaction of n gravitons with the effective particle worldline, as shown in Fig. 2(a). The curly line denotes a two-point function $D_{\alpha\beta\gamma'\delta'}^{ab}$ of the metric perturbation (i.e. of a graviton). The straight line denotes the effective point particle. We remark that from the point of view of the gravitons, the particle acts as an external source that couples to the metric perturbations. As such, the straight line in Fig. 2(a) does not represent the physical propagation of the compact object but acts as an external field, which is determined in the end via the consistent solution to the particle equations of motion.

The power counting of n gravitons interacting with the effective particle is given by

$$\text{Fig. (2a)} = iS_{pp}^{(n)} \sim \frac{m}{m_{\text{pl}}^n} d\tau h^n \sim \varepsilon \left(\frac{L}{\varepsilon}\right)^{1-(n/2)}. \quad (3.28)$$

The self-interaction vertices that result from the nonlinearity of the Einstein-Hilbert action are given in Fig. 2(b). The power counting for the self-interaction of n gravitons

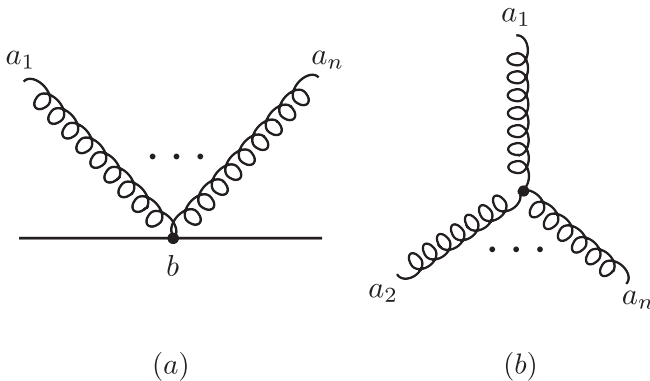


FIG. 2. Interaction vertices. Diagram (a) shows the interaction vertex for n gravitons, denoted by curly lines, coupling to a point particle, denoted by a straight line. Diagram (b) shows the self-interaction vertex of n gravitons. The labels a_1, a_2, \dots and b are CTP indices, which take values of \pm .

gives

$$\text{Fig. (2b)} = iS^{(n)} \sim m_{\text{pl}}^2 d^4x \nabla^2 \frac{h^n}{m_{\text{pl}}^n} \sim \left(\frac{L}{\varepsilon}\right)^{1-(n/2)}. \quad (3.29)$$

From Table I we see that the power counting indicates that every type of interaction term involving any number of gravitons scales as L^p where $p \leq 1$.

C. Feynman rules and calculating the effective action

We now turn to calculating the effective action from (3.18) for $J_a^{\mu\nu} = 0$. Standard quantum field theory arguments [50–52] demonstrate that the effective action is given by

$$\begin{aligned} i\Gamma[\langle z_{1,2}^\mu \rangle] &= iS_{pp}^{(0)}[\langle z_1^\mu \rangle] - iS_{pp}^{(0)}[\langle z_2^\mu \rangle] \\ &+ (\text{sum of all 1PI connected diagrams}). \end{aligned} \quad (3.30)$$

By “connected diagrams” we mean those contiguous diagrams constructed using the Feynman rules for the interaction terms in (3.11). By “1PI connected diagrams” we mean those connected diagrams that are one-particle-irreducible [51,52]. However, we are only interested in those connected diagrams that contribute at the classical level since the quantum corrections due to graviton loops on the motion of an astrophysical body are utterly negligible. Therefore, the effective point particle worldline is assumed to be totally decohered and we will simply represent the expectation value of the worldline coordinates operators $\langle \hat{z}_a^\mu \rangle$ by their semiclassical values z_a^μ .

A diagram with ℓ graviton loops scales as $L^{1-\ell}$, in units where $\hbar = 1$. Therefore, classical processes correspond to those diagrams that scale linearly with L (i.e., tree-level diagrams) and provide the dominant contributions to the effective action so that

$$\begin{aligned} i\Gamma[z_{1,2}] &= iS_{pp}^{(0)}[z_1] - iS_{pp}^{(0)}[z_2] \\ &+ (\text{sum of all tree-level connected diagrams}) \\ &+ \dots \end{aligned} \quad (3.31)$$

In this manner we have a systematic method for computing the self-force equations order by order in ε .

The relationship between the connected diagrams, the interaction terms, and the power counting is provided by the Feynman rules so that, given a diagram at a given order in ε , we can translate these into mathematical expressions. The Feynman rules are the following:

- (1) A vertex represents the particle-field interaction $iV_{ppa_1 \dots a_n}^{(n)\alpha_1 \dots \beta_n}$ or the graviton self-interaction $iV_{a_1 \dots a_n}^{(n)\alpha_1 \dots \beta_n}$ as appropriate.
- (2) Include a factor of the graviton two-point function $D_{\alpha\beta\gamma'\delta'}^{ab}(x, x')$ connecting vertices labeled by CTP indices a and b at spacetime points x and x' .

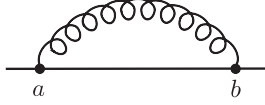


FIG. 3. The diagram contributing to the first-order self-force described by the MST-QW equation.

- (3) Include a factor of $D_{\alpha\beta\gamma'\delta'}^{-a}(x, x')$ for each graviton that propagates from the worldline at event x' with CTP index a to the *field* point x .
- (4) Sum over all CTP indices and integrate over all spacetime for each vertex.
- (5) Divide by the appropriate symmetry factor, S .

The symmetry factor S for a particular diagram is found by counting the number of ways one can permute the internal CTP indices while retaining the same set of propagators appearing in the diagram. We will show how these rules are implemented as we continue.

To derive the MST-QW self-force equation, we only need those diagrams that contribute at $O(\varepsilon L)$. From the Feynman rules for the interactions in Fig. 2 it follows that there is only one such diagram at this order, which is shown in Fig. 3. Therefore, the effective action to first order in ε is

$$i\Gamma[z_{1,2}] = -im \int d\tau_1 + im \int d\tau_2 + \text{Fig.}(3) + O(\varepsilon^2 L), \quad (3.32)$$

where

$$\text{Fig.}(3) = \left(\frac{1}{2}\right) iV_{pp}^{(1)\alpha\beta} \cdot D_{\alpha\beta\gamma'\delta'}^{ab} \cdot iV_{pp}^{(1)\gamma'\delta'} \cdot b. \quad (3.33)$$

The symmetry factor here is $1/2$ and

$$V_{pp-}^{(1)\alpha\beta} \equiv V_{pp}^{(1)\alpha\beta}[z_1] - V_{pp}^{(2)\alpha\beta}[z_2] \quad (3.34)$$

$$V_{pp+}^{(1)\alpha\beta} \equiv \frac{1}{2}(V_{pp}^{(1)\alpha\beta}[z_1] + V_{pp}^{(2)\alpha\beta}[z_2]), \quad (3.35)$$

where $V_{pp}^{(1)\alpha\beta}$ is essentially the point particle stress tensor given in (3.5).

According to (3.19), only those terms linear in $z^\mu = z_1^\mu - z_2^\mu$ contribute to the equations of motion so that expanding $V_{pp\pm}^{(1)\alpha\beta}$ through $O(z_-)$ gives

$$\begin{aligned} i\Gamma[z_{\pm}] &= -im \int d\tau z^\mu g_{\mu\alpha} a_+^\alpha \\ &+ \frac{im^2}{2m_{\text{pl}}^2} \int d\tau \int d\tau' z^\mu(\tau) w_\mu^{\alpha\beta\nu}[z_+^\alpha] \\ &\times \nabla_\nu D_{\alpha\beta\gamma'\delta'}^{\text{ret}}(z_+^\alpha, z_+^{\alpha'}) \dot{z}_+^{\gamma'} \dot{z}_+^{\delta'} + O(z_-^2). \end{aligned} \quad (3.36)$$

Here the 4-acceleration is

$$a_+^\mu(\tau) = \frac{Dz_+^\mu}{d\tau}, \quad (3.37)$$

τ is the proper time associated with the worldline described

by z_+^α so that

$$g_{\alpha\beta}(z_+) \dot{z}_+^\alpha \dot{z}_+^\beta = -1, \quad (3.38)$$

and the tensor $w^{\mu\alpha\beta\nu}[z]$ is defined by

$$w^{\mu\alpha\beta\nu} = \frac{1}{2} u^\alpha u^\beta w^{\mu\nu} - w^{\mu(\alpha} u^{\beta)} u^\nu \quad (3.39)$$

$$w^{\mu\nu} = g^{\mu\nu} + u^\mu u^\nu. \quad (3.40)$$

Notice that the Hadamard two-point function $D_{\alpha\beta\gamma'\delta'}^H$ does not enter at $O(z_-)$ and can consistently be ignored when deriving the classical equations of motion for the CO since it always appears at higher orders in z^μ .

We observe that the retarded propagator in (3.36) is divergent when $\tau' = \tau$. In order to have a finite and well-behaved force on the compact object from the metric perturbations, we will need to regularize this divergence and possibly renormalize the appropriate couplings of the theory.

D. Regularization of the leading order self-force

The CS-EFT approach is founded in the theory of quantum fields in curved spacetime [50,53]. The renormalization of divergences in this context has received much attention over the decades and a considerable body of techniques has been developed to remove these divergences in a systematic and self-consistent manner. We therefore find it natural to renormalize the divergence in (3.36) using these methods even if they are somewhat unfamiliar in classical gravitational problems.

Of these approaches the method of dimensional regularization [54] is particularly useful. This regularization scheme preserves the general coordinate and gauge symmetries of the theory but is also a natural choice to use within an effective field theory framework [9,55,56].

From (3.36) we may write the divergent integral

$$\begin{aligned} I^\mu(\tau) &= \int_{-\infty}^{\infty} d\tau' w^{\mu\alpha\beta\nu} \nabla_\nu D_{\alpha\beta\gamma'\delta'}^{\text{ret}}(z_+^\mu, z_+^{\mu'}) u_+^{\gamma'} u_+^{\delta'} \\ &\equiv \int_{-\infty}^{\infty} d\tau' \Delta^\mu(\tau, \tau') \end{aligned} \quad (3.41)$$

as the sum of a regular and divergent contribution,

$$\begin{aligned} I^\mu(\tau) &= Fp \int_{-\infty}^{\infty} d\tau' \Delta^\mu(\tau, \tau') + \int_{-\infty}^{\infty} d\tau' \Delta_{\text{div}}^\mu(\tau, \tau') \\ &= I_{\text{fin}}^\mu(\tau) + I_{\text{div}}^\mu(\tau), \end{aligned} \quad (3.42)$$

where Fp denotes the finite part of the divergent integral in the sense of Hadamard [57]. We refer the reader to Appendix B for our notations and definitions regarding distribution theory as well as to the excellent texts of [58,59].

To calculate the finite and divergent parts we write the proper time integral as

$$I^\mu(\tau) = \left(\int_{-\infty}^{\tau_{<}} + \int_{\tau_{<}}^{\tau_{>}} + \int_{\tau_{>}}^{\infty} \right) d\tau' w^{\mu\alpha\beta\nu} \nabla_\nu \times D_{\alpha\beta\gamma'\delta'}^{\text{ret}}(z_+^\alpha, z_+^{\alpha'}) u_+^{\gamma'} u_+^{\delta'}, \quad (3.43)$$

where $\tau_{<}/>$ denotes the values of proper time when the worldline enters/leaves the normal convex neighborhood of $z_+^\mu(\tau)$. Using Hadamard's construction for the retarded propagator [57,60], the second integral can be written as

$$\int_{\tau_{<}}^{\tau_{>}} d\tau' w^{\mu\alpha\beta\nu} \nabla_\nu [\theta(\tau - \tau') \Delta^{1/2} \delta(\sigma(z^\alpha, z^{\alpha'})) u_+^\alpha u_+^\beta + \theta(\tau - \tau') V_{\alpha\beta\gamma'\delta'}(z^\alpha, z^{\alpha'}) u_+^{\gamma'} u_+^{\delta'}], \quad (3.44)$$

where $V_{\alpha\beta\gamma'\delta'}(x, x')$ is a regular function, $\Delta(x, x')$ is the van Vleck determinant, and $\sigma(x, x')$ is Synge's world function. See [60] for further details about Hadamard's construction. The divergent contribution to $I^\mu(\tau)$ therefore arises solely from the first integral in (3.44) and we may write the finite part as

$$I_{\text{fin}}^\mu(\tau) = \lim_{\epsilon \rightarrow 0} \int_{-\infty}^{\tau - \epsilon} d\tau' w^{\mu\alpha\beta\nu} \nabla_\nu D_{\alpha\beta\gamma'\delta'}^{\text{ret}}(z_+^\alpha, z_+^{\alpha'}) u_+^{\gamma'} u_+^{\delta'} \quad (3.45)$$

upon recalling that the retarded propagator vanishes for $\tau' > \tau$.

The divergent part of $I^\mu(\tau)$ can be extracted using a momentum space representation for the graviton propagator that is initially introduced by Bunch and Parker for a scalar field in an arbitrary curved spacetime in [37]. We show in [39] that the retarded propagator is given in Riemann normal coordinates (RNC) by

$$D_{\hat{a}\hat{b}\hat{c}\hat{d}}^{\text{ret}}(y) = \Delta^{1/2}(y) \int_{\mathcal{C}} \frac{d^d k}{(2\pi)^d} e^{ik \cdot y} \left[\frac{P_{\hat{a}\hat{b}\hat{c}\hat{d}}(\eta)}{k^2} + \dots \right], \quad (3.46)$$

where $y^{\hat{a}}$ denotes the RNC of $z^\alpha(\tau')$ with respect to the origin at $z^\alpha(\tau)$, \mathcal{C} is the appropriate contour for the retarded propagator, and

$$P_{\hat{a}\hat{b}\hat{c}\hat{d}}(\eta) = \frac{1}{2} \left(\eta_{\hat{a}\hat{c}} \eta_{\hat{b}\hat{d}} + \eta_{\hat{a}\hat{d}} \eta_{\hat{b}\hat{c}} - \frac{2}{d-2} \eta_{\hat{a}\hat{b}} \eta_{\hat{c}\hat{d}} \right). \quad (3.47)$$

The terms in (3.46) given by $+\dots$ contribute to the coincidence limit expansion of $V_{\alpha\beta\gamma'\delta'}(x, x')$, as we demonstrate in [39], and are already included in (3.45). We therefore identify the divergent part of $I^\mu(\tau)$ with

$$I_{\text{div}}^{\hat{m}}(\tau) = w^{\hat{m}\hat{a}\hat{b}\hat{c}} P_{\hat{a}\hat{b}\hat{c}\hat{d}} u^{\hat{d}} \int_{-\infty}^{\infty} d\tau' \partial_{\hat{n}} \times \left[\Delta^{1/2}(y) \int_{\mathcal{C}_{\text{ret}}} \frac{d^d k}{(2\pi)^d} \frac{e^{ik \cdot y}}{k^2} \right]. \quad (3.48)$$

We provide the computational details in Appendix C and show that

$$I_{\text{div}}^\mu(\tau) = 0. \quad (3.49)$$

Having regularized the leading order contribution to the effective action in Fig. 3 we use the variational principle

$$\left. \frac{\delta \Gamma[z_\pm]}{\delta z_\pm^\mu(\tau)} \right|_{z_- = 0, z_+ = z} = 0 \quad (3.50)$$

to give the self-force on a compact object moving in a vacuum background spacetime,

$$a^\mu(\tau) = \frac{m}{2m_{\text{pl}}^2} w^{\mu\alpha\beta\nu} \lim_{\epsilon \rightarrow 0} \int_{-\infty}^{\tau - \epsilon} d\tau' \nabla_\nu D_{\alpha\beta\gamma'\delta'}^{\text{ret}}(z^\alpha, z^{\alpha'}) u^{\gamma'} u^{\delta'}, \quad (3.51)$$

which was originally derived by Mino, Sasaki and Tanaka [40] and by Quinn and Wald [41].

IV. MATCHING AND FINITE SIZE EFFECTS

We outline a matching procedure for fixing the non-minimal couplings c_E, c_B, \dots , which contain information about the internal structure of the compact object. We also determine the lowest order at which the finite size of the compact object affects its motion via tidal deformations induced by the background curved geometry. Using coordinate invariant arguments we demonstrate that such finite size effects from a small Schwarzschild black hole or neutron star unambiguously enter the self-force at $O(\epsilon^5)$ and as deviations from a point particle motion at $O(\epsilon^4)$. We also discuss the tidal deformations of a white dwarf star, which are more sensitive to the curvature of the background geometry.

A. Nonspinning black holes and neutron stars

To begin we recall the effective point particle action given in (2.4). The coefficients $c_{E,B}$ are parameters that depend upon the internal structure of the extended body. We must therefore match the effective point particle theory onto the full theory in order to encode this microscopic or ‘‘high-energy’’ structure onto the long-wavelength effective theory.

The matching procedure involves calculating (coordinate invariant) observables in both the effective theory and the full theory [61]. By expanding the observable of the full theory in the long-wavelength limit, where the effective theory is applicable, we can simply read off the values of $c_{E,B}$ as well as any other coefficients in (2.4).

Consider the amplitude for Compton graviton scattering shown in Fig. 4, which represents the scattering of gravitational waves in the spacetime of the isolated compact object. Power counting this amplitude in the effective point particle theory gives

$$i\mathcal{A} \sim \dots \& \frac{c_{E,B}}{m_{\text{pl}}^2} \left(\frac{1}{\mathcal{R}^2} \right)^2 \& \dots, \quad (4.1)$$

where the $1/\mathcal{R}^2$ comes from the two spacetime covariant

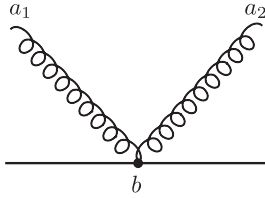


FIG. 4. Graviton scattering off the background of a static and spherically symmetric extended body (e.g., a Schwarzschild black hole, a nonspinning neutron star).

derivatives in the background Riemann tensor and the $\&$ denotes “and a term that scales as.” While the cross section includes contributions from other terms in the effective particle action, it will contain one term proportional to $c_{E,B}^2$,

$$\sigma_{pp} \sim |i\mathcal{A}|^2 \sim \dots \& \frac{c_{E,B}^2}{m_{\text{pl}}^4} \frac{1}{\mathcal{R}^8} \& \dots, \quad (4.2)$$

where the pp subscript indicates that this is the cross section computed in the effective point particle theory.

We turn now to the scattering cross section in the full theory. A cross section represents an effective scattering area and the only scale present in the full theory of the isolated compact object is set by its size $r_m \sim m/m_{\text{pl}}^2$. It follows that

$$\sigma_{\text{full}} = r_m^2 F\left(\frac{r_m}{\mathcal{R}}\right), \quad (4.3)$$

where F is a dimensionless function that can be computed directly using conventional methods. In the long-wavelength limit where $r_m/\mathcal{R} \ll 1$, the cross section will contain a term proportional to \mathcal{R}^{-8} ,

$$\sigma_{\text{full}} \sim \dots \& r_m^2 \left(\frac{r_m}{\mathcal{R}}\right)^8 \& \dots. \quad (4.4)$$

Since quantities computed in the effective theory ought to match those computed in the long-wavelength limit of the full theory, we conclude that

$$c_{E,B} \sim m_{\text{pl}}^2 r_m^5 \sim \frac{m^5}{m_{\text{pl}}^8} \quad (4.5)$$

upon identifying the \mathcal{R}^{-8} terms in both σ_{pp} and σ_{full} .

The first diagram that the finite size terms will contribute is proportional to $c_{E,B}$ and is shown in Fig. 5(a). This describes the deviation from the pure point particle motion experienced by the compact object due to the inclusion of the nonminimal couplings to the background spacetime, which scales with ε as

$$\text{Fig. (5a)} \sim c_{E,B} d\tau \left(\frac{1}{\mathcal{R}^2}\right)^2 \sim \varepsilon^4 L \quad (4.6)$$

and enters at fourth order.

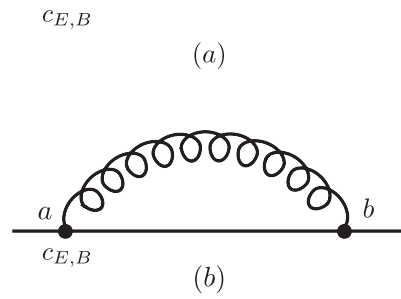


FIG. 5. Lowest order contributions to (a) deviation from (minimal) point particle motion due to the tidal deformations of the compact object, and (b) the self-force from the interaction of gravitational radiation with these deformations.

This diagram does not couple to metric perturbations; it persists in the absence of gravitational radiation. As a result, while Fig. 5(a) will affect the motion of the particle it is not a correction to the self-force. To find the order at which the tidal deformations affect the self-force we power count the diagram in Fig. 5(b) to find that

$$\text{Fig. (5b)} \sim c_{E,B} d\tau \left(\frac{1}{\mathcal{R}^2}\right)^2 \frac{h}{m_{\text{pl}}} \sqrt{\varepsilon L} \sim \varepsilon^5 L. \quad (4.7)$$

Finite size effects therefore enter the self-force at fifth order in ε .

B. Nonspinning white dwarf stars

In (4.5) we assume that the size of the compact object is of the same order as its mass, $r_m \sim m/m_{\text{pl}}^2$. While this holds true for black holes and neutron stars it does not for white dwarf (WD) stars. WDs are thousands of times larger than their Schwarzschild radius and subsequently experience stronger tidal effects than a black hole (BH) or neutron star (NS) with the same mass. In fact, the tides may be so severe that the WD is tidally disrupted at some point along its orbit about the SMBH. As a result, we expect that finite size effects may be (numerically) enhanced and alter the WD’s motion, possibly at a lower order in ε .

To see how this can arise, we define the ratio of the compact object’s radius to its mass by f_{co} so that

$$r_m = f_{\text{co}} Gm = \frac{f_{\text{co}}}{32\pi} \frac{m}{m_{\text{pl}}^2} \quad (4.8)$$

and the bookkeeping parameter ε becomes

$$\varepsilon \equiv \frac{r_m}{\mathcal{R}} \sim f_{\text{co}} \frac{m}{m_{\text{pl}}^2 \mathcal{R}} \quad (4.9)$$

with $m/m_{\text{pl}} \sim \sqrt{\varepsilon L/f_{\text{co}}}$. If the compact object is a black hole then $f_{\text{bh}} = 2$. For a neutron star having a mass of $1.4M_{\odot}$ and a radius between 10 and 16 km, it follows that f_{ns} varies between 4.8 and 7.7, respectively.

Using the new expressions for r_m and ε , it is not difficult to show that

$$c_{E,B} \sim f_{\text{co}}^5 \frac{m^5}{m_{\text{pl}}^8} \sim m_{\text{pl}}^2 r_m^5 \quad (4.10)$$

and therefore the leading order finite size effects from induced tides scales as

$$\text{Fig.}(5a) \sim f_{\text{co}} \varepsilon^4 L. \quad (4.11)$$

Since $\varepsilon \propto f_{\text{co}}$ it follows that Fig. 5(a) scales as f_{co}^5 . We remark that this observation agrees with that in [62,63] where the authors observe that the induced quadrupole moment of a neutron star scales as r_{ns}^5 .

The parameter ε generally depends on some distance scale, r , set by the orbit of the compact object. As a result, ε takes on different values at different orbital scales. Similarly, in the post-Newtonian expansion the small parameter (the relative velocity of the compact objects v) depends upon the scale of the orbital separation r through the virial theorem, $v(r) \sim (Gm/r)^{1/2}$.

To determine how the leading order finite size effects from Fig. 5(a) depend on the orbital scale r , we consider the SMBH background to be a Schwarzschild black hole. It then follows from (1.1) and (4.9) that

$$\varepsilon = \frac{r_m}{R} = 2^{3/4} 3^{1/4} f_{\text{co}} \frac{m}{M} \left(\frac{r}{M} \right)^{-3/2}. \quad (4.12)$$

As the orbital scale decreases we observe that ε increases.

For a WD, ε can be significantly larger than for a BH or NS with the same mass because f_{wd} is typically much larger than both f_{bh} and f_{ns} . In fact, f_{wd} can be so large that Fig. 5(a) may be *numerically enhanced* and important at orders in ε lower than the naive fourth order estimation given in the previous section. Such enhancement is consistent with our physical intuition that a WD experiences stronger tidal deformations than a BH or NS with the same mass.

To demonstrate this enhancement consider a simple example. Assume that the radius of the WD equals the Schwarzschild radius of the nonspinning SMBH it orbits. Choosing the radii to be 600 km each, it follows that the masses of the WD and SMBH are $m \approx 0.6M_{\odot}$ [64] and $M = 4000M_{\odot}$, respectively. For these values, (4.8) indicates that

$$f_{\text{wd}} \approx 6750, \quad (4.13)$$

which is much larger than both f_{bh} and f_{ns} , as expected.

For this scenario, how do the leading order finite size effects of (4.11) change with the orbital scale, r , of the WD? Figure 6 shows a log-log plot of $f_{\text{wd}} \varepsilon^4$ as a function of the radial distance r/M from the SMBH. The dark line is $f_{\text{wd}} \varepsilon^4$ while the dashed gray lines are plots of ε^s for $s = 0, \dots, 4$. As the orbital scale decreases, the dark line crosses several dashed gray lines indicating that Fig. 5(a) is numerically enhanced from the naive ε^4 estimate for BH's and NS's to order ε^s because of the stronger WD tidal deformations. It is the scaling of the nonminimal

couplings $c_{E,B}$ in (4.10) with the fifth power of f_{wd} that is responsible for this enhancement of the leading order finite size effects.

However, this enhancement cannot proceed indefinitely. If the tidal deformations become strong enough to transfer material from the WD to the SMBH (via Roche lobe overflow) or to disintegrate the WD at its Roche limit, then the WD is tidally disrupted and can no longer be described effectively as a point particle. This indicates that our particular construction of a point mass effective field theory will no longer satisfactorily describe the binary.

Using Newtonian estimates we find the Roche limit for the rigid (fluid) WD to be near $r \approx 24M$ ($r \approx 47M$). These scales are represented by a triangle (circle) in Fig. 6. The WD's Roche lobe begins to overflow and transfer mass that accretes onto the SMBH when $r \approx 40M$ [65] and is denoted with a square in Fig. 6. In all three cases the WD is tidally disrupted, a process that occurs near the $s = 2$ line.

All of this suggests that finite size effects from induced tidal deformations can be enhanced for a WD until the star undergoes tidal disruption at $O(\varepsilon^2)$. If one is interested in calculating the second order self-force on a WD these tidal effects may have to be taken into account at some point during the binary's evolution to accurately determine the gravitational waveforms.

If the SMBH mass is increased to $10^5 M_{\odot}$, we estimate that tidal disruption occurs much closer to the SMBH's horizon. Describing the WD as an effective point particle is therefore valid over much of its orbital evolution. Increasing the mass of the SMBH further, we find that WD tidal disruption occurs inside the event horizon and is therefore ignorable with respect to observables and processes outside of the SMBH. Therefore, for the SMBH masses relevant for LISA's bandwidth the tidal disruption

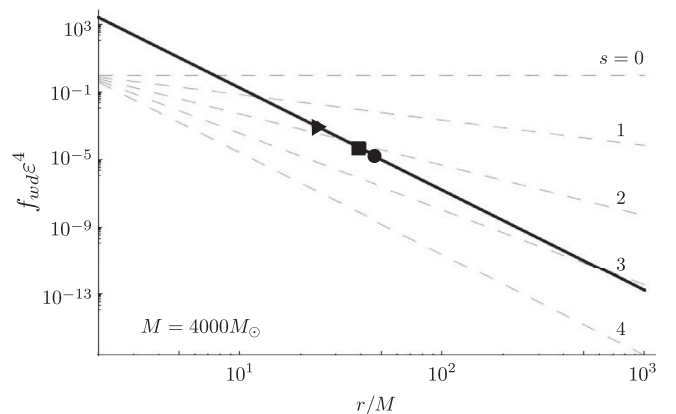


FIG. 6. The effects from the finite size of a white dwarf star can be enhanced as it orbits in closer to the SMBH. The white dwarf seems to undergo some form of tidal disruption by either tidal disintegration (triangle and circle) or Roche lobe overflow (square). In either case, tidal disruption may be numerically equivalent to a second order process.

of WDs is likely to be negligible except perhaps near the plunge and merger phases for a $\lesssim 10^5 M_\odot$ Schwarzschild SMBH.

If the WD is tidally disrupted before it plunges into the SMBH, one can conceivably construct a new EFT that is valid at scales much larger than the orbital scale of the binary in which the SMBH, the WD, and the mass transferring to the SMBH are treated collectively as an effective point particle. Given the complexity of such a system an EFT description would be very useful. However, the matching procedure to determine the large number of relevant nonminimal couplings is likely to be difficult given that high order intrinsic multipoles will need to be included to accurately describe this system.

We recapitulate our results from this section with an explicit statement of the effacement principle for *nonspinning* compact objects.

Effacement principle for EMRIs.—Tidally induced moments will affect the acceleration of a compact object at $O(\varepsilon^4)$.

For a white dwarf orbiting a Schwarzschild SMBH this effect may be numerically enhanced until the star undergoes tidal disruption at $O(\varepsilon^2)$, which may be relevant when the SMBH mass is less than about $10^5 M_\odot$ for the particular example discussed here.

V. CONCLUSION

We develop an effective field theory approach for systematically deriving the self-force on a compact object moving in an arbitrary curved spacetime without the slow motion or weak field restrictions. The EFT is a realization of the open quantum system paradigm in systems with a large scale separation such that the system's induced fluctuations from the backreaction of the coarse-grained quantum field is utterly negligible [8]. An initial value formulation of quantum field theory is adopted here using the closed-time-path (CTP) formalism for the in-in generating functional, which guarantees real and causal equations of motion for the compact object. As an illustration of the procedures involved in our approach, we showed how to derive the MST-QW equation describing the (first-order) self-force on a compact object.

We describe the compact object as an effective point particle that is capable of accounting for tidally induced finite size effects. In calculating the effective action we encounter ultraviolet divergences stemming from a point particle interacting with arbitrarily high frequency modes of a graviton field. Using Hadamard's *partie finie* to isolate the nonlocal finite part from the quasilocal divergences, we are able to implement dimensional regularization within a (quasilocal) momentum space representation for the graviton propagator [39]. As such, all power divergences can be immediately set to zero implying that only logarithmic divergences are relevant for renormalizing the parameters

of the theory. At first order, the effective action naively contains a power divergence that identically vanishes.

In the spirit of an effacement principle, we find that the finite size of the compact object first affects its motion at $O(\varepsilon^4)$ for a nonspinning black hole and neutron star. For a white dwarf star we deduce that such effects may be enhanced until the white dwarf is tidally disrupted at $O(\varepsilon^2)$ in which case the effective point particle description, and, in particular, the effective field theory developed here, breaks down. One may conceivably construct a new effective field theory by treating the supermassive black hole, the white dwarf, and the accreting mass as an effective point particle possessing many relevant nonminimal couplings to the background geometry describing the intrinsic moments of this composite object.

The leading order finite size corrections cause a deviation from the motion of a minimally coupled point particle that is not caused by interactions with gravitons but is due to the torques that develop on the tidally deformed compact object. On the other hand, the self-force is affected by the induced moments of the compact object at $O(\varepsilon^5)$.

In summary, the EFT approach has at least two major advantages over the existing approaches: It provides a systematic procedure for carrying out a perturbative treatment, and an economical way to treat the ultraviolet divergences. Our CS-EFT improves on the PN-EFT introduced in [10] in that it is valid for a general curved spacetime and not limited to slow motion or weak field conditions. These will prove to be of special benefit for higher order self-force calculations. We will apply these steps to calculate the self-force at second order in ε [12], the gravitational radiation emitted by EMRIs [13], and the self-force on spinning compact objects [14].

ACKNOWLEDGMENTS

We thank Eanna Flanagan, Eric Poisson, Cole Miller, Alessandra Buonanno, and Ted Jacobson for useful questions and comments. C. R. G. is gratefully indebted to Ira Rothstein for an invitation to the Workshop on Effective Field Theory Techniques in Gravitational Wave Physics, where much of this work had its origins. He also thanks Ira Rothstein, Walter Goldberger, and Adam Leibovich for invaluable discussions during and after the workshop. This work is supported in part by NSF Grant No. PHY-0601550.

APPENDIX A: DEFINITIONS AND RELATIONS FOR THE QUANTUM TWO-POINT FUNCTIONS

In this Appendix we collect some definitions, identities, and relations for the quantum two-point functions that are relevant for this work.

The positive and negative frequency Wightman functions are defined as

$$G_{\alpha\beta\gamma'\delta'}^+(x, x') = \langle \hat{h}_{\alpha\beta}(x) \hat{h}_{\gamma'\delta'}(x') \rangle \quad (\text{A1})$$

$$G_{\alpha\beta\gamma'\delta'}^-(x, x') = \langle \hat{h}_{\gamma'\delta'}(x') \hat{h}_{\alpha\beta}(x) \rangle, \quad (\text{A2})$$

respectively. The angled brackets represent the quantum expectation value of the operator \hat{O} so that

$$\langle \hat{O} \rangle \equiv \text{Tr}[\hat{\rho}(\Sigma_i) \hat{O}] \quad (\text{A3})$$

and $\hat{\rho}(\Sigma_i)$ is the density matrix of the quantum field given on a hypersurface Σ_i at constant coordinate time $x^0 = t_i$.

The Feynman, Dyson, Hadamard, and commutator (also known as the Pauli-Jordan function or the causal function) two-point functions are, respectively,

$$G_{\alpha\beta\gamma'\delta'}^F(x, x') = \langle T \hat{h}_{\alpha\beta}(x) \hat{h}_{\gamma'\delta'}(x') \rangle \quad (\text{A4})$$

$$G_{\alpha\beta\gamma'\delta'}^D(x, x') = \langle T^* \hat{h}_{\alpha\beta}(x) \hat{h}_{\gamma'\delta'}(x') \rangle \quad (\text{A5})$$

$$G_{\alpha\beta\gamma'\delta'}^H(x, x') = \langle \{ \hat{h}_{\alpha\beta}(x), \hat{h}_{\gamma'\delta'}(x') \} \rangle \quad (\text{A6})$$

$$G_{\alpha\beta\gamma'\delta'}^C(x, x') = \langle [\hat{h}_{\alpha\beta}(x), \hat{h}_{\gamma'\delta'}(x')] \rangle, \quad (\text{A7})$$

where T is the time-ordering operator and T^* is the anti-time-ordering operator. The field commutator is independent of the particular state used to evaluate it. Given the Wightman functions in (A1) and (A2), we write the above two-point functions in the form (ignoring the tensor indices from here on)

$$G_F(x, x') = \theta(t - t') G_+(x, x') + \theta(t' - t) G_-(x, x') \quad (\text{A8})$$

$$G_D(x, x') = \theta(t' - t) G_+(x, x') + \theta(t - t') G_-(x, x') \quad (\text{A9})$$

$$G_H(x, x') = G_+(x, x') + G_-(x, x') \quad (\text{A10})$$

$$G_C(x, x') = G_+(x, x') - G_-(x, x'). \quad (\text{A11})$$

From these we define the retarded and advanced propagators by

$$-iG_{\text{ret}}(x, x') = \theta(t - t') G_C(x, x') \quad (\text{A12})$$

$$+iG_{\text{adv}}(x, x') = \theta(t' - t) G_C(x, x'). \quad (\text{A13})$$

These propagators also satisfy the following useful identities:

$$-iG_{\text{ret}}(x, x') = G_F(x, x') - G_-(x, x') \quad (\text{A14})$$

$$= G_+(x, x') - G_D(x, x') \quad (\text{A15})$$

$$iG_{\text{adv}}(x, x') = G_D(x, x') - G_-(x, x') \quad (\text{A16})$$

$$= G_+(x, x') - G_F(x, x') \quad (\text{A17})$$

from which the Feynman propagator can be written in

terms of its real and imaginary parts as

$$G_F(x, x') = -\frac{i}{2} \left[G_{\text{ret}}(x, x') + G_{\text{adv}}(x, x') \right] - \frac{1}{2} G_H(x, x'). \quad (\text{A18})$$

The Feynman, Dyson, and Wightman functions are not all independent since

$$G_H(x, x') = G_F(x, x') + G_D(x, x') \quad (\text{A19})$$

$$= G_+(x, x') + G_-(x, x'). \quad (\text{A20})$$

Under the interchange of x and x' the Feynman, Dyson, and Hadamard two-point functions are symmetric, the commutator is antisymmetric, and

$$G_+(x, x') = G_-(x', x) \quad (\text{A21})$$

$$G_{\text{ret}}(x, x') = G_{\text{adv}}(x', x). \quad (\text{A22})$$

APPENDIX B: DISTRIBUTIONS, PSEUDOFUNCTIONS, AND HADAMARD'S FINITE PART

In this Appendix we present the basic structure, concepts, and definitions of distribution theory that are relevant for this work. The reader is referred to [58,59] for more information.

Consider the set of functions ϕ that are infinitely smooth C^∞ and have compact support on any finite interval. These functions, called *testing* or *test functions*, form a set \mathcal{D} . A *functional* f is a mapping that associates a complex number to every testing function in \mathcal{D} . A *distribution* is a linear and continuous functional on the space of test functions \mathcal{D} and is frequently denoted by the symbols $\langle f, \phi \rangle$ and f .

For a locally integrable function $f(t)$, we can associate a natural distribution through the convergent integral

$$\langle f, \phi \rangle \equiv \int_{-\infty}^{\infty} dt f(t) \phi(t) \quad (\text{B1})$$

for some testing function $\phi \in \mathcal{D}$. Notice that we are using the same symbol to denote both the distribution and the function that generates the distribution. This is an example of a regular distribution. All distributions that are not regular are *singular distributions* and will be our main concern in the rest of this Appendix. An example of a singular distribution is the well-known delta functional δ .

Often, a singular distribution gives rise to a singular integral, which can be written in terms of its divergent and finite parts. For the purposes of clarity and illustration, it is best to consider a simple example. Let us compute the integral

$$\left\langle \frac{\theta(t)}{t}, \phi \right\rangle = \int_0^{\infty} dt \frac{\phi(t)}{t} \quad (\text{B2})$$

for $\phi(t)$ a testing function in \mathcal{D} and $\theta(t)$ the step, or

Heaviside, function. This integral is obviously divergent since $1/t$ is not a locally integrable function at the origin. Nevertheless, we may extract the finite part (in the sense of Hadamard [57]) of the integral by isolating the divergences from the finite terms.

To this end we write

$$\phi(t) = \phi(0) + t\psi(t), \quad (\text{B3})$$

where $\psi(t)$ is a continuous function for all t . Putting this into (B2) and integrating gives

$$\left\langle \frac{\theta(t)}{t}, \phi \right\rangle = \lim_{\epsilon \rightarrow 0^+} \left[\phi(0) \log b - \phi(0) \log \epsilon + \int_{\epsilon}^b dt \psi(t) \right], \quad (\text{B4})$$

where we assume that the testing function $\phi(t)$ vanishes for $t \geq b$ for some real number b . The finite part of (B2) is defined to be the remainder upon subtracting off the divergent contribution(s). In this case, dropping the $\log \epsilon$ term gives the finite part of the integral

$$Fp \int_0^{\infty} dt \frac{\phi(t)}{t} = \phi(0) \log b + \int_0^{\infty} dt \psi(t), \quad (\text{B5})$$

where the symbol Fp denotes the Hadamard finite part of the integral. Therefore, the divergent part of the integral is given by $-\phi(0) \log \epsilon$.

A distribution that generates the finite part of the integral is called a *pseudofunction*, which we now calculate for this example. Inserting (B3) into the finite part (B5) gives

$$Fp \int_0^{\infty} dt \frac{\phi(t)}{t} = \lim_{\epsilon \rightarrow 0^+} \left[\int_{\epsilon}^{\infty} dt \frac{\phi(t)}{t} + \phi(0) \log \epsilon \right]. \quad (\text{B6})$$

Since

$$\phi(0) = \int_{-\infty}^{\infty} dt \delta(t) \phi(t) = \langle \delta, \phi \rangle, \quad (\text{B7})$$

it follows that the finite part can be written as an integral of a distribution with a testing function

$$Fp \int_0^{\infty} dt \frac{\phi(t)}{t} = \lim_{\epsilon \rightarrow 0^+} \int_{\epsilon}^{\infty} dt \left[\frac{1}{t} + \delta(t) \log \epsilon \right] \phi(t), \quad (\text{B8})$$

which defines the pseudofunction,

$$Pf \frac{\theta(t)}{t} = \frac{\theta(t)}{t} + \delta(t) \lim_{\epsilon \rightarrow 0^+} \log \epsilon. \quad (\text{B9})$$

Therefore, the finite part of the integral generates a pseudofunction (a regular distribution) that yields a finite value when integrated with a testing function,

$$\int_{-\infty}^{\infty} dt Pf \frac{\theta(t)}{t} \phi(t) = Fp \int_{-\infty}^{\infty} dt \frac{\theta(t)}{t} \phi(t). \quad (\text{B10})$$

Quite generally, the value that the distribution assigns to a testing function will have a divergent part consisting of both power divergences and powers of logarithmically diverging terms so that

$$I(\epsilon) = \sum_{p=1}^N \frac{a_p}{\epsilon^p} + \sum_{p=1}^M b_p \log^p \epsilon \quad (\text{B11})$$

for some appropriate integers N, M . This form for $I(\epsilon)$ is related to the so-called Hadamard's ansatz [57] and appears often in regularizing divergent quantities involving two-point functions of a quantum field in curved spacetime [50,53].

APPENDIX C: DIVERGENT PART OF EFFECTIVE ACTION

In this Appendix we give the explicit calculation of the divergent part of the $O(\epsilon)$ effective action. In Riemann normal coordinates, $y^{\hat{a}}$ describes the coordinate of a point x' relative to the origin at x and is defined in terms of a tetrad $e_{\alpha}^{\hat{a}}$ at x through

$$y^{\hat{a}} = -e_{\alpha}^{\hat{a}}(x) \sigma^{\alpha}(x, x'). \quad (\text{C1})$$

Here $\sigma(x, x')$ is Synge's world function, which numerically equals half the squared geodesic interval between x and x' , and $\sigma^{\alpha} \equiv \sigma^{;\alpha}$ is proportional to the vector at x that is tangent to the unique geodesic connecting x and x' . See [60] for further details. Let us equate the points x and x' with $z_{+}^{\mu}(\tau)$ and $z_{+}^{\mu}(\tau')$, respectively, on the leading order (i.e., geodesic) particle worldline.

The arbitrariness of the tetrad at x implies that we may choose

$$e_{\alpha}^{\hat{0}}(\tau) = -u_{+\alpha}(\tau) \quad (\text{C2})$$

if we maintain the condition $e_{\alpha}^{\hat{a}} e_b^{\alpha} = \delta_b^{\hat{a}}$. Hence, the particle's 4-velocity is orthogonal to the components of the tetrad in the spatial directions, $e_{\alpha}^{\hat{i}} u_{+}^{\alpha} = 0$ where $\hat{i} = 1, \dots, d-1$. Using these relations and (C1), the Riemann normal coordinate representation of the point $x' = z_{+}^{\mu}(\tau')$ on the geodesic worldline is given by

$$y^{\hat{a}} = e_{\alpha}^{\hat{a}}(\tau) u_{+}^{\alpha}(\tau) (\tau - \tau') = \delta_{\hat{0}}^{\hat{a}} (\tau - \tau') \quad (\text{C3})$$

implying that

$$k \cdot y = k_{\hat{a}} y^{\hat{a}} = -k^{\hat{0}} (\tau - \tau'). \quad (\text{C4})$$

With $s = \tau' - \tau$ the divergent integral in (3.48) is

$$I_{\text{div}}^{\hat{m}}(\tau) = \frac{1}{2} \frac{d-3}{d-2} w^{\hat{m}\hat{n}} \int_{-\infty}^{\infty} ds \int_{\mathcal{C}} \frac{d^d k}{(2\pi)^d} \frac{e^{ik^0 s}}{k^2} \times [ik_{\hat{n}} \Delta^{1/2} + \partial_{\hat{n}} \Delta^{1/2}]. \quad (\text{C5})$$

In RNC, the square root of the van Vleck determinant and its derivative for a *vacuum* background spacetime is given by

$$\Delta^{1/2}(y(s)) = g^{-1/4}(y(s)) = 1 + O(s^4) \quad (\text{C6})$$

$$\partial_{\hat{n}} \Delta^{1/2}(y(s)) = O(s^3), \quad (\text{C7})$$

where the higher order terms yield contributions to (C5) that scale as $\sim k^{d-6}$ and do not contribute since these are ultraviolet finite in four dimensions. Integrating (C5) over s gives

$$I_{\text{div}}^{\hat{m}}(\tau) = \frac{i}{2} \frac{d-3}{d-2} w^{\hat{m}\hat{i}} \int_{-\infty}^{\infty} \frac{d^{d-1}k}{(2\pi)^{d-1}} \frac{k_{\hat{i}}}{k^2} \quad (\text{C8})$$

from which it follows that the spatial momentum integral

vanishes identically. Therefore, (C5) vanishes and

$$I_{\text{div}}^{\mu}(\tau) = e_{\hat{m}}^{\mu}(\tau) I_{\text{div}}^{\hat{m}}(\tau) = 0, \quad (\text{C9})$$

as claimed. No parameters are renormalized at this order in perturbation theory since the naively divergent quantities are actually zero.

-
- [1] C.R. Galley and B.L. Hu, Phys. Rev. D **72**, 084023 (2005).
 - [2] C.R. Galley, B.L. Hu, and S.Y. Lin, Phys. Rev. D **74**, 024017 (2006).
 - [3] C.R. Galley, Ph.D. thesis, University of Maryland, 2007.
 - [4] P. Johnson and B.L. Hu, Phys. Rev. D **65**, 065015 (2002).
 - [5] P. Johnson and B.L. Hu, Found. Phys. **35**, 1117 (2005).
 - [6] P. Johnson, Ph.D. thesis, University of Maryland, 1999.
 - [7] M. Gell-Mann and J.B. Hartle, Phys. Rev. D **47**, 3345 (1993).
 - [8] E. Calzetta and B.L. Hu, Phys. Rev. D **55**, 3536 (1997).
 - [9] C.P. Burgess, Annu. Rev. Nucl. Part. Sci. **57**, 329 (2007).
 - [10] W. Goldberger and I. Rothstein, Phys. Rev. D **73**, 104029 (2006).
 - [11] In addition to [1,2,10] for applying effective field theory techniques to the motion of extended bodies and charges, see also [66], which briefly mentions using a closely related approach for extreme mass ratio inspirals.
 - [12] C.R. Galley, “Second order self-force for extreme mass ratio inspirals using a curved spacetime effective field theory approach” (unpublished).
 - [13] C.R. Galley, “Gravitational waves for extreme mass ratio inspirals using a curved spacetime effective field theory approach” (unpublished).
 - [14] C.R. Galley, “Self-force on a spinning compact object using a curved spacetime effective field theory approach” (unpublished).
 - [15] The LISA website is <http://lisa.nasa.gov>.
 - [16] See <http://www.cco.caltech.edu/esp/lisa/lisatab.html> for a comprehensive list of sources potentially detectable by LISA.
 - [17] B.F. Whiting, J. Math. Phys. (N.Y.) **30**, 1301 (1989).
 - [18] We define the Ricci tensor as $R_{\mu\nu} = \partial_{\alpha}\Gamma_{\mu\nu}^{\alpha} - \partial_{\nu}\Gamma_{\mu\alpha}^{\alpha} + \dots$ and the metric has mostly positive signature $(-, +, +, +)$.
 - [19] See Sec. IV for more details concerning a white dwarf, which has a typical radius $r_{\text{wd}} \sim 10^3 m/m_{\text{pl}}^2$.
 - [20] R. A. Porto, Phys. Rev. D **73**, 104031 (2006).
 - [21] R. A. Porto and I. Z. Rothstein, Phys. Rev. Lett. **97**, 021101 (2006).
 - [22] R. A. Porto, in *Proceedings of the 11th Marcel Grossman Meeting on General Relativity*, edited by H. Kleinert, R. T. Jantzen, and R. Ruffini (World Scientific, Singapore, 2008).
 - [23] R. A. Porto and I. Z. Rothstein, arXiv:0712.2032.
 - [24] W. Goldberger and I. Rothstein, Phys. Rev. D **73**, 104030 (2006).
 - [25] R. A. Porto, Phys. Rev. D **77**, 064026 (2008).
 - [26] W. Goldberger, in *Particle Physics and Cosmology: The Fabric of Spacetime*, Lecture Notes of the Les Houches Summer School Vol. LXXXVI, edited by F. Bernardeau, C. Grojean, and J. Dalibard (Elsevier Science, The Netherlands, 2007).
 - [27] R. A. Porto and R. Sturani, in *Particle Physics and Cosmology: The Fabric of Spacetime*, Ref. [26].
 - [28] W. D. Goldberger and I. Z. Rothstein, Gen. Relativ. Gravit. **38**, 1537 (2006).
 - [29] The effective field theory approach has also been used in [67] to derive the radiation-reaction force on an electrically charged extended body interacting with its own electromagnetic radiation, generalizing the Abraham-Lorentz-Dirac equation for a point charge. It can also be derived from a stochastic field theory perspective, which contains EFT. See [4–6].
 - [30] For a concrete example in the explication of this point, compare [68] to [35] on the cosmological particle creation backreaction problem.
 - [31] J. Schwinger, J. Math. Phys. (N.Y.) **2**, 407 (1961).
 - [32] L. V. Keldysh, Zh. Eksp. Teor. Fiz. **47**, 1515 (1964) [Sov. Phys. JETP **20**, 1018 (1965)].
 - [33] G. Zhou, Z. Su, B. Hao, and L. Yu, Phys. Rep. **188**, 1 (1985).
 - [34] R. D. Jordan, Phys. Rev. D **33**, 444 (1986).
 - [35] E. Calzetta and B.L. Hu, Phys. Rev. D **35**, 495 (1987).
 - [36] E. Calzetta and B.L. Hu, Phys. Rev. D **37**, 2878 (1988).
 - [37] T. S. Bunch and L. Parker, Phys. Rev. D **20**, 2499 (1979).
 - [38] B.L. Hu and D.J. O’Connor, Phys. Rev. D **30**, 743 (1984).
 - [39] C.R. Galley, “Propagators in curved spacetime: A momentum space representation using Feynman diagrams” (unpublished).
 - [40] Y. Mino, M. Sasaki, and T. Tanaka, Phys. Rev. D **55**, 3457 (1997).
 - [41] T.C. Quinn and R.M. Wald, Phys. Rev. D **56**, 3381 (1997).
 - [42] A. Einstein, L. Infeld, and B. Hoffmann, Ann. Math. **39**, 65 (1938).
 - [43] L. Blanchet, Living Rev. Relativity **9** (2006) 051.
 - [44] We will introduce spin and determine the influence it has on the effective particle’s motion in a forthcoming paper [14].

- [45] H. D. Politzer, Nucl. Phys. **B172**, 349 (1980).
- [46] H. Georgi, Nucl. Phys. **B361**, 339 (1991).
- [47] L. D. Faddeev and V. N. Popov, Phys. Lett. **25B**, 29 (1967).
- [48] P. A. M. Dirac, *Lectures on Quantum Mechanics* (Yeshiva University, New York, 1964).
- [49] Actually, it is the classical particle action, $-m \int d\tau$, that scales as $m\mathcal{R}$. However, for nearly circular geodesics the orbital angular momentum L scales as $m\mathcal{R}$. For historical reasons, we will continue to label $m\mathcal{R}$ by L .
- [50] N. D. Birrell and P. C. W. Davies, *Quantum Fields in Curved Space* (Cambridge University Press, Cambridge, England, 1986).
- [51] M. E. Peskin and D. V. Schroeder, *An Introduction to Quantum Field Theory* (Harper Collins, Reading, MA, 1995).
- [52] L. E. Ryder, *Quantum Field Theory* (Cambridge University Press, Cambridge, England, 1999), 2nd ed.
- [53] R. M. Wald, *Quantum Field Theory in Curved Spacetime and Black Hole Thermodynamics* (The University of Chicago Press, Chicago, 1994).
- [54] G. 't Hooft and M. Veltman, Nucl. Phys. **B44**, 189 (1972).
- [55] A. V. Manohar, arXiv:hep-ph/9606222.
- [56] I. Z. Rothstein, arXiv:hep-ph/0308266.
- [57] J. Hadamard, *Lectures on Cauchy's Problem in Linear Partial Differential Equations* (Yale University Press, New Haven, 1923).
- [58] L. Schwartz, *Théorie des Distributions, Tomes I et II* (Hermann, Paris, 1957).
- [59] A. H. Zemanian, *Distribution Theory and Transform Analysis* (Dover Publications, Inc., New York, 1987).
- [60] E. Poisson, Living Rev. Relativity **7** (2004) 024.
- [61] Strictly speaking, one can use any quantity for the matching procedure but it is simpler to draw coordinate invariant conclusions by matching with a coordinate invariant quantity, such as a scattering amplitude, a cross section, etc.
- [62] E. E. Flanagan and T. Hinderer, Phys. Rev. D **77**, 021502 (2008).
- [63] K. S. Thorne, Phys. Rev. D **58**, 124031 (1998).
- [64] S. L. Shapiro and S. A. Teukolsky, *Black Holes, White Dwarfs, and Neutron Stars* (Wiley, New York, 1983).
- [65] P. P. Eggleton, Astrophys. J. **268**, 368 (1983).
- [66] B. Kol and M. Smolkin, Phys. Rev. D **77**, 064033 (2008).
- [67] A. Leibovich, Report at the Workshop on Effective Field Theory Techniques in Gravitational Wave Physics, Carnegie Mellon University, 2007.
- [68] J. B. Hartle and B. L. Hu, Phys. Rev. D **20**, 1772 (1979).